Integrated Co-Electrolysis and Syngas Methanation for the Direct Production of Synthetic Natural Gas from CO_2 and H_2O

Chalachew Mebrahtu[+],[a] Markus Nohl[+],[b, c] Lucy Dittrich,[b, c] Severin R. Foit,[b] L. G. J. (Bert) de Haart,[b] Rüdiger-A. Eichel,*[b, c] and Regina Palkovits*[a]

The concept of an integrated power-to-gas (P2G) process was demonstrated for renewable energy storage by converting renewable electrical energy to synthetic fuels. Such a dynamically integrated process enables direct production of synthetic natural gas (SNG) from CO_2 and H_2O. The produced SNG can be stored or directly injected into the existing natural gas network. To study process integration, operating parameters of the high-temperature solid oxide electrolysis cell (SOEC) producing syngas (H_2+CO) mixtures through co-electrolysis and a fixed bed reactor for syngas methanation of such gas mixtures were first optimized individually. Reactor design, operating conditions, and enhanced SNG selectivity were the main targets of the study. SOEC experiments were performed on state-of-the-art button cells. Varying operating conditions (temperature, flow rate, gas mixture and current density) emphasized the capability of the system to produce tailor-made syngas mixtures for downstream methanation. Catalytic syngas methanation was performed using hydrotalcite-derived 20%Ni-2%Fe/(Mg,Al)O_x catalyst and commercial methanation catalyst (Ni/Al_2O_3) as reference. Despite water in the feed mixture, SNG with high selectivity ($\geq$90%) was produced at 300 °C and atmospheric pressure. An adequate rate of syngas conversion was obtained with H_2O contents up to 30%, decreasing significantly for 50% H_2O in the feed. Compared to the commercial catalyst, 20%Ni-2%Fe/(Mg,Al)O_x enabled a higher rate of CO_x conversion.

Introduction

Fossil fuels depletion, increasing CO_2 emissions, and global warming are some of the global challenges today's society is facing. Sustainable technologies are an essential element in transforming these challenges into opportunities. Renewable energy (RE) market shares such as solar power and wind turbines are increasing worldwide in order to shift towards a "low-carbon" and sustainable energy economy.[1–3] These technologies offer a huge potential; however, they are intermittent by nature and the energy produced will not always fulfill the demand. Therefore, optimized energy storage is crucial for a smooth transition from fossil fuels to renewable energy sources.[4–6] Among the emerging technologies, power-to-gas (P2G) is considered as a route to transform energy into gases that can be stored and transported more easily than electrical power. Moreover, P2G enables valorizing CO_2 for the production of synthetic natural gas (SNG) and other value-added chemicals tackling both CO_2 recycling and RE storage.[7–9]

Conventional CO_2 conversion involves a three-step process: (i) H_2 production by water electrolysis, (ii) H_2/CO_2 gas mixture equilibration by the reverse water-gas shift reaction (RWGS) and (iii) hydrogenation of CO_2 under stationary conditions, for example, via methanation or Fischer-Tropsch chemistry. However, these three successive steps are unfavourable to adapt to the intermittent nature of RE sources. Hence, a separate H_2 storage/transport step is usually required.[7,10–13] Accordingly, P2G technologies facilitate operating under intermittent electrical power supply. Herein, we present a conceptual study on integrating high-temperature CO_2 and H_2O co-electrolysis with syngas methanation (Figure 1). The integration concept is based on the design of a reactor unit, which enables direct generation of SNG by dynamically coupling high-temperature co-electrolysis and syngas methanation. Such an integrated route bears a high potential as a future element for sustainable RE storage due to reduced downstream process steps and adaptability to the dynamic nature of RE generation.

[a] Dr. C. Mebrahtu,[+] Prof. Dr. R. Palkovits
Lehrstuhl für Heterogene Katalyse und Technische Chemie
Institut für Technische und Makromolekulare Chemie (ITMC)
RWTH Aachen University
Worringerweg 2, 52074 Aachen (Germany)
E-mail: Palkovits@itmc.rwth-aachen.de
[b] M. Nohl,[+] L. Dittrich, S. R. Foit, Dr. L. G. J. (Bert) de Haart, Prof. Dr. R.-A. Eichel
Institut für Energie- und Klimaforschung Grundlagen der Elektrochemie (IEK-9)
Forschungszentrum Jülich
52425 Jülich (Germany)
E-mail: r.eichel@fz-juelich.de
[c] M. Nohl,[+] L. Dittrich, Prof. Dr. R.-A. Eichel
Institut für Physikalische Chemie
RWTH Aachen University
52074 Aachen (Germany)
[+] These authors contributed equally to this work.

Supporting information for this article is available on the WWW under https://doi.org/10.1002/cssc.202002904

This publication is part of a Special Collection highlighting "The Latest Research from our Board Members". Please visit the Special Collection at https://bit.ly/cscBoardMembers.

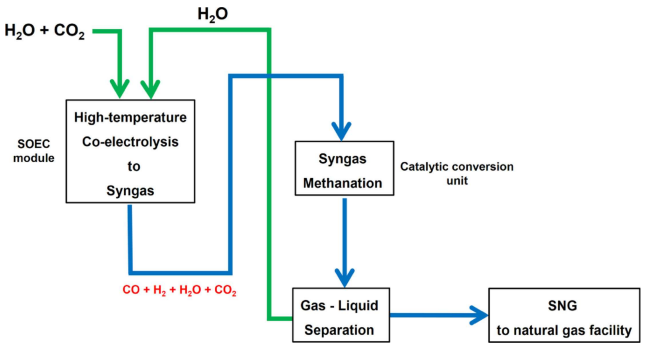

Figure 1. Integrated P2G process for synthetic natural gas (SNG) production from CO_2 and H_2O.

Additionally, thermal integration, balancing the exothermic (syngas methanation) and endothermic (co-electrolysis) processes creates an energy-efficient storage solution. In a typical integrated P2G process, for a direct generation of SNG from CO_2 and H_2O, various reactions can occur. Equations (1)–(4), therefore, summarize possible reactions involved in the process [Eq. (2) is mainly valid for the conversion of CO_2 to CO in the co-electrolysis cell].

High-temperature co-electrolysis (idealized overall reaction) in the solid oxide electrolysis cell (SOEC):

$$CO_2 + H_2O \rightarrow CO + H_2 + O_2 \quad (1)$$

RWGS reaction in the SOEC:

$$CO_2 + H_2 \rightarrow CO + H_2O \quad (2)$$

Methanation reactions in the fixed-bed reactor:

$$CO_2 + 4H_2 \rightarrow CH_4 + 2H_2O \quad (3)$$

$$CO + 3H_2 \rightarrow CH_4 + H_2O \quad (4)$$

Generally, such integrated P2G processes are preferable compared to their conventional counterparts due to the special advantage of high-temperature co-electrolysis to produce tailor-made syngas compositions and adjust the H_2/CO ratio.[14–18] Additionally, in the second step, the syngas generated by co-electrolysis can be directly converted to SNG via methanation. To date, only few reports are available on the direct SNG production from CO_2 and H_2O using different types of electrochemical reactors.[19–24] Recently, some contributions were published focusing on simulation-based results for integrated P2G process towards one-step SNG production. Among these studies are in situ SNG production using SOECs under low-temperature operations,[25] overall efficiency comparison of reversible SOECs with sub-surface storage of CO_2 and CH_4 with respect to pumped hydro,[26] and P2G efficiency of reversible SOECs aiming for grid stabilization applications.[27] Nevertheless, to the best of our knowledge, an integrated P2G process operating under dynamic conditions with aim of higher SNG production and selectivity has not yet been reported. Major challenges of an integrated P2G process are the design and balanced operation conditions as SOEC and syngas methanation are favored at different reaction temperatures. In addition, developing a system easily adaptable to a fluctuating RE supply presents a vital task.

Herein, we present the concept of an integrated P2G process combining co-electrolysis and SNG production under dynamic reaction conditions. High-temperature SOEC based on a commercial CeramTec cell and syngas methanation applying a novel hydrotalcite derived catalyst were investigated. Both setups were optimized separately to establish best operating conditions for the concept of integration. Furthermore, representative feed mixtures were used in the methanation process to demonstrate new insights on the combination of both process steps.

High-temperature co-electrolysis of H_2O and CO_2 enables adapting to almost any desired syngas ratio or more precisely output composition for further downstream processes. Hereby, it is not necessary to install intermediate process steps as this is the case for, for example, the low-temperature electrolysis pathways.[9] The faradaic efficiency of the conversion of H_2O and CO_2 to H_2 and CO at high temperatures is close to 100% since competing reactions are negligible.[18] Therefore, high overall system efficiencies can be achieved, especially for the case of usage of the heat from the exothermic methanation for water evaporation, which is the most energy-demanding process.[28] For electrolysis, high temperatures increase efficiency regarding the required electrical power and demand, since a large portion of energy for electrolysis is provided as heat.[29]

Results and Discussion

Syngas production: high-temperature CO_2 and H_2O co-electrolysis

The possibility to tailor syngas compositions by high-temperature co-electrolysis has been shown in our previous work.[18] Analysis of the fuel side gas stream shows an almost linear dependence between feed gas ratio of H_2O:CO_2 to the product ratio of H_2:CO. A 3:1 H_2O:CO_2 mixture will also result in a 3:1 H_2:CO mixture. With increasing current density this ratio is slightly pushed towards hydrogen. The flow rate itself determines the fuel utilization at a given current density.[18] The performance analyses of co-electrolysis at various H_2O:CO_2 ratios are presented in the Supporting Information (Figure S10).

In parallel to the experiments, a theoretical model based on thermodynamics was developed to predict the output gas composition based on the operating parameters including initial composition, temperature, current density and flow rate. The results of the theoretical calculations showed a good agreement with the experimental results.[18]

As a proof of concept, we demonstrate the solver algorithm with a comparison of experimental data taken by mass spectrometry in Figure 2. The measurement was performed at 825 °C with a flow rate of 2 $L \cdot h^{-1}$. The input composition was

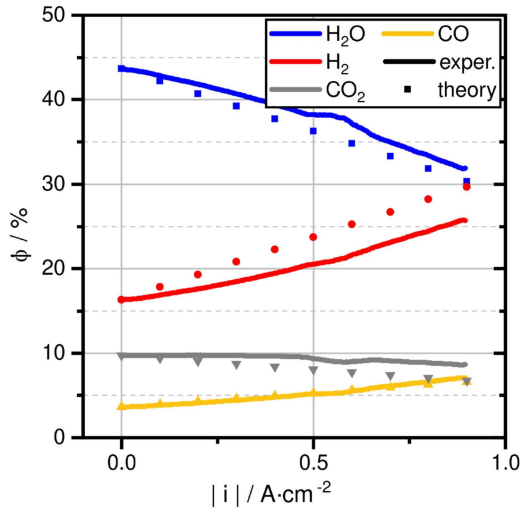

Figure 2. Partial pressure of gas species as a function of current density as measured in experiment and compared to a theoretical model.

chosen to 13.3% CO_2 + 20% H_2 + 40% H_2O with N_2 as balance (H_2 is required to prevent reoxidation of the nickel electrode; 20% was used as a standard and comparison to previously conducted measurements and could be lowered to a minimum of 5%). The current density was recorded up to 0.9 $A \cdot cm^{-2}$. In Figure 2, the experimental values (solid lines) of the partial pressure for each species expressed in shares are plotted against the current density. Values from theoretical calculations are added (dots) in order to prove correctly predicted trends for output compositions from the solver when comparing to experiment.

Since renewable energy sources provide a fluctuating electrical power, the electrolysis operating conditions need to be adjusted to result in a constant output syngas composition. The described model is used to calculate possible operating conditions to obtain the output syngas composition that is required for methanation. The input gas stream for methanation was set to: 1.5% CO_2, 12.5% CO, 56% H_2, 10% H_2O and 20% N_2 as balance (see section on syngas methanation). This reverse engineering avoids many time-consuming trials in experiments. Calculations were performed for a fuel (CO_2 + H_2O) conversion of (80 ± 3)%. Table 1 lists a selection of possible co-electrolysis operating conditions (input gas composition, current density, temperature and flow rate), which all result in the methanation input gas composition. It does not matter that a first equilibration by RWGS takes place at the specified temperature since the fuel content is thereby not altered.

The results presented in Table 1 show that the desired feed gas for the follow-up methanation can be obtained under various conditions. The numbers for initial composition, temperature, current density, flow rate and output composition result from reverse-engineering. The cell voltages originate from experiments with similar conditions with respect to temperature and thus represent an estimate. All further power indications are calculated from current density and cell voltage. The reference case to the consumption of one kWh is indicated by 100% dissipated electrical power in form of supplied energy. All numbers are rounded to the first digit.

The results in Table 1 also illustrate the capability of co-electrolysis to anticipate to fluctuations in the available renewable power. For five distinct cases ranging from 35 to 125% of dissipated electrical power, the corresponding output gas available for methanation has almost similar compositions. Thus, a change in available power for co-electrolysis does not alter the output syngas composition, when the appropriate operating conditions are selected. This mostly involves changing the current density and temperature for co-electrolysis. The experiments (Figure 2) also show that a change in current density results in a relatively constant syngas ratio, which shows the possible dynamic operation of co-electrolysis. Which operating conditions are preferred should be the outcome of a full process engineering analysis of combined co-electrolysis and methanation, in which for instance also the heat integration is included. This analysis is, however, beyond the scope of this contribution.

Syngas methanation

Based on their superior performance, a hydrotalcite-derived Ni-based catalyst [i.e., 20%Ni-2%Fe/(Mg,Al)O_x] and a commercial Ni/Al_2O_3 methanation catalyst were used as selected materials for syngas methanation. The hydrotalcite-derived catalyst was

Table 1. Selection of operating conditions for the co-electrolysis process that are capable to produce the required syngas mixtures for the methanation process.

Initial composition [%]					T	Current density	Cell voltage	Power density	Dissipated electrical power	Flow rate	Output composition [%]				
CO_2	CO	H_2	H_2O	N_2	[°C]	[$A \cdot cm^{-2}$]	[V]	[$W \cdot cm^{-2}$]	[% of 1 kWh]	[$L \cdot h^{-1}$]	CO_2	CO	H_2	H_2O	N_2
14.0	0.0	30.0	36.0	20.0	900	1.1	1.00	1.10	35	1.0	1.6	12.4	57.7	8.3	20.0
14.0	0.0	28.0	38.0	20.0	900	2.3	1.23	2.83	100	2.0	1.5	12.5	57.1	8.9	20.0
14.0	0.0	23.0	43.0	20.0	875	2.5	1.37	3.43	125	2.0	1.8	12.2	56.0	10.0	20.0
14.0	0.0	21.0	45.0	20.0	850	1.3	1.15	1.50	50	1.0	1.9	12.1	56.3	9.7	20.0
14.0	0.0	26.0	40.0	20.0	825	2.4	–	–	–	2.0	1.8	12.2	57.2	8.8	20.0
14.0	0.0	16.0	50.0	20.0	800	1.4	1.41	1.97	75	1.0	2.4	11.6	55.5	10.5	20.0
14.0	0.0	25.0	41.0	20.0	775	1.2	–	–	–	1.0	2.2	11.8	57.0	9.0	20.0
14.0	0.0	19.0	47.0	20.0	750	1.3	–	–	–	1.0	2.6	11.4	56.4	9.6	20.0
14.0	0.0	7.0	59.0	20.0	725	1.6	–	–	–	1.0	3.2	10.8	54.6	11.4	20.0
14.0	0.0	16.0	50.0	20.0	700	1.4	–	–	–	1.0	3.1	10.9	56.2	9.8	20.0

prepared by co-precipitation method as described in our previous work[30,31] and used in syngas methanation. The as-synthesized catalyst is a $(Mg,Al)O_x$-supported Ni–Fe catalyst with an active metal loading of 20% Ni and 2% Fe on a basic support (55% Mg and 23% Al). The as-prepared material was rigorously characterized using different techniques such as X-ray diffraction (XRD), H_2 temperature-programmed reduction (H_2–TPR), CO_2 temperature-programmed desorption (CO_2–TPD), scanning electron microscopy (SEM), and scanning transmission electron microscopy (STEM). All the characterization results are provided in the Supporting Information (Figures S2–S6 and Table S1). Reaction conditions for CO_x methanation were chosen based on the relevance for industrial implementation. Therefore, all reactions were performed at 300 °C and atmospheric pressure. To investigate the rate of CO_x conversion and valorize the results as reference points, methanation reactions were performed using a stoichiometric mixture of H_2:(CO_2 + CO) = 4:1. CO concentration was varied to simulate a partial electrolysis of CO_2, while H_2O was considered as fully electrolyzed. CO fractions of 5, 10, and 20% were introduced (Figure 3). The rate of CO_x conversion increased with increasing CO fraction in the feed. This enhanced activity indicates CO as an important intermediate of the main reaction.

The second part of the experiments focused on the effect of H_2O on CO_2 methanation. Different mixture compositions with a total feed ratio of (H_2 + H_2O):CO_2 = 4:1 were introduced at 300 °C and 1 atm. Figure 4 summarizes the results obtained using 20%Ni-2%Fe/$(Mg,Al)O_x$ upon varying H_2O fractions between 10, 30, and 50%. The rate of CO_2 conversion decreased upon increasing H_2O fraction in the feed mixture.

Figure 5 illustrates the results of CO_x methanation for feed mixtures potentially resulting from co-electrolysis under dynamic conditions. In both cases, CO_x was converted to SNG with a selectivity exceeding ≥95%. The overall CO_x conversion rate slightly increased with increasing CO fraction, but the SNG selectivity slightly decreased from ≥97% in the feed mixture with 5% CO to about 95% for a feed containing 10% CO. This might be due to water gas shift reaction, which is favorable at higher CO fractions and in presence of water in the feed.[32,33]

To further elucidate the effect of CO fraction on catalytic CO_x conversion, CO methanation was performed in presence of different water fractions (Figure 6).

The findings in the case of CO as sole carbon source also explain the results observed in CO_x methanation of feed mixtures obtained by the full conversion of CO_2 to CO and

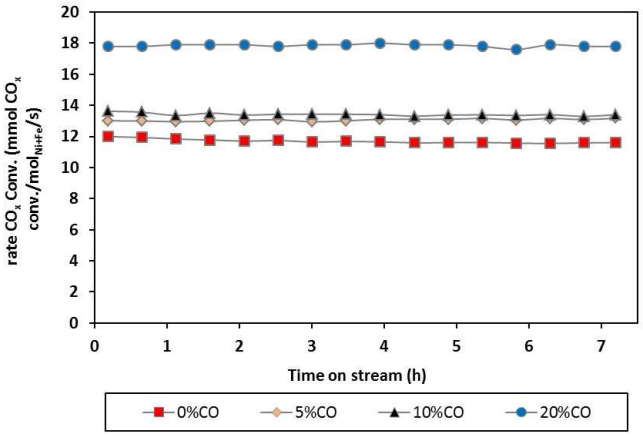

Figure 3. Effect of CO fraction on the reference reaction (CO_2 methanation) over 20%Ni-2%Fe/$(Mg,Al)O_x$ at 300 °C, 1 atm and gas hourly space velocity (GHSV) = 5017 h^{-1}.

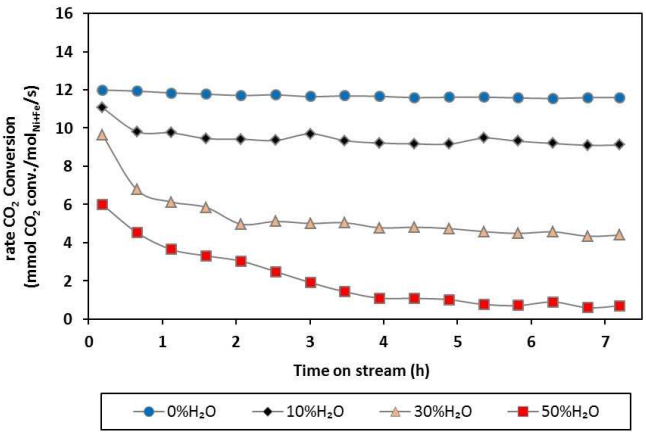

Figure 4. Effect of H_2O fraction on CO_2 methanation over 20%Ni-2%Fe/$(Mg,Al)O_x$ at 300 °C, 1 atm and GHSV = 5017 h^{-1}.

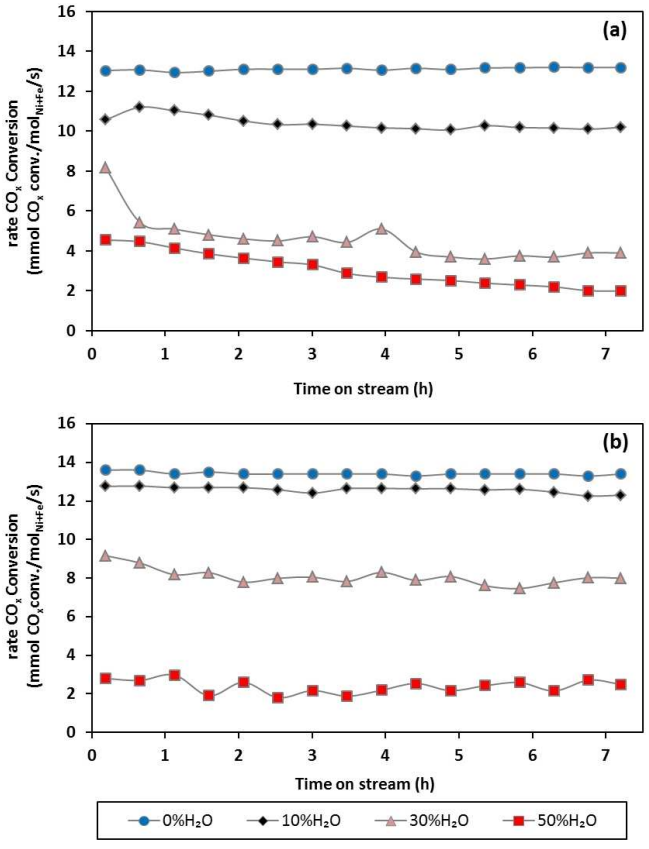

Figure 5. Catalytic CO_x methanation over 20%Ni-2%Fe/$(Mg,Al)O_x$ at 300 °C, 1 atm and GHSV = 5017 h^{-1}. Effect of water on different feed mixtures: (a) 11% CO_2 + 5% CO and (b) 6% CO_2 + 10% CO.

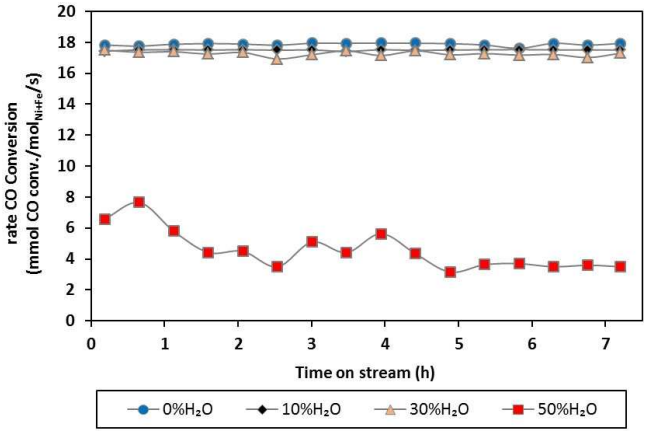

Figure 6. Effect of water on catalytic CO methanation over 20%Ni-2%Fe/(Mg,Al)O_x at 300 °C, 1 atm, and GHSV = 5017 h^{-1}.

partial electrolysis of H_2O. Without CO_2 and H_2O in the feed mixture and using 20%Ni-2%Fe/(Mg,Al)O_x as a catalyst, the rate of CO conversion reached 17.9 mmol CO conv. mol^{-1}_{Ni+Fe} s^{-1}. In the presence of H_2O, the rate of CO conversion and SNG selectivity decreased and CO_2 formation (with selectivity up to 10%) occurred. We suggest that the water gas shift reaction presents the major explanation for this effect.

On the other hand, at all the reaction conditions investigated, the two catalysts exhibited distinct differences in CO_x methanation activity, while the selectivity to SNG reached 90–100%, according to the superior methanation activity of Ni-based catalysts. Indeed, the hydrotalcite-derived material facilitated a significantly higher rate of CO_x conversion compared to the commercial methanation catalyst (Figure 7), which is 2–4 times higher with lower H_2O fractions in the feed. Higher catalytic performance of 20%Ni-2%Fe/(Mg,Al)O_x than the conventional Ni/Al_2O_3 commercial catalyst is possibly due to the improved basic sites, metal dispersion and formation of a Ni–Fe alloy, which was found to be more active than monometallic Ni.[30,34]

The development of thermally stable catalysts with higher activity for low-temperature CO_x methanation is still a challenge mainly due to deactivation at reaction conditions. The deactivation of Ni-based catalysts can be due to oxidation of Ni^0, sintering and coke deposition under reaction conditions.[35] Hence, appropriate regeneration strategies of Ni-based catalysts are crucial to use the same catalytic bed for a longer time under dynamic reaction conditions. Therefore, spent 20%Ni-2%Fe/(Mg,Al)O_x catalyst, after testing for one week under dynamic

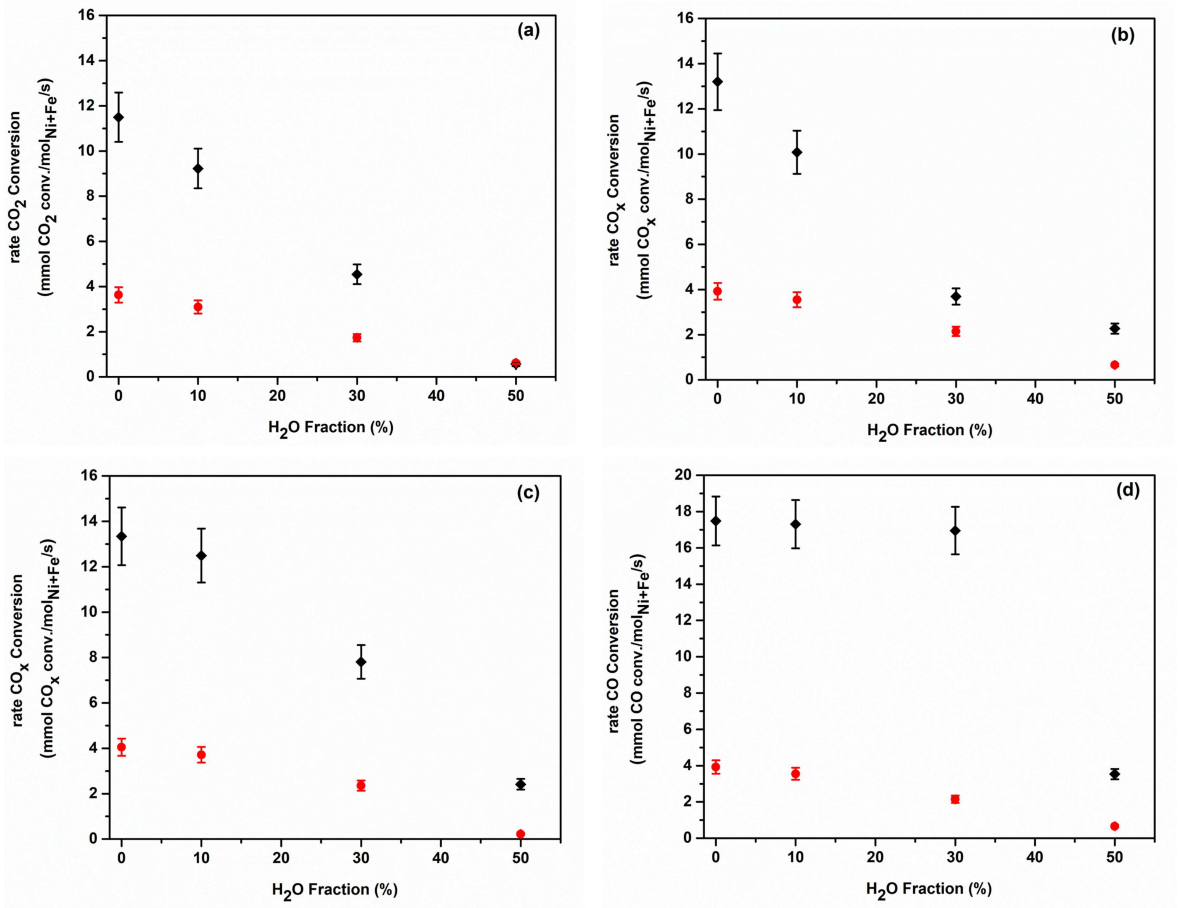

Figure 7. Effect of water on catalytic CO_x methanation: activity comparison between (♦) 20%Ni-2%Fe/(Mg,Al)O_x and (●) commercial methanation catalysts at 300 °C, 1 atm, and GHSV = 5017 h^{-1}. (a) CO_2 methanation, (b) 11% CO_2 + 5% CO, (c) 6% CO_2 + 10% CO, and (d) CO methanation.

conditions, was regenerated and its activity was retested. The regeneration methods used were drying for several hours (under N_2 flow) and re-reduction for 2 h at 600 °C (under H_2 flow). Figure 8 shows the trends for both regeneration strategies compared to the fresh 20%Ni-2%Fe/(Mg,Al)O_x catalyst at 300 °C and atmospheric pressure. After drying, the catalyst showed up to 30% loss in activity while re-reduction enabled full recovery of the initial catalytic performance in the reaction mixtures investigated.

The full recovery of the activity after re-reduction indicates that the main cause for catalyst deactivation could be oxidation of the Ni^0 species at the reaction conditions used (i.e., higher H_2O content in the feed mixture) because, in CO_x methanation, water is known as a weak oxidizing agent at temperatures $\geq$300 °C.[36,37]

To the greater context, the results obtained by the afore-demonstrated concept of coupled P2G process validate a possible integration of two steps (co-electrolysis and syngas methanation) for a higher rate of CO_x conversion and SNG selectivity by decreasing further downstream processes. In this work, the dynamic behavior of renewable energy generation was simulated by continuously varying the feed mixture introduced to the methanation reactor.

The overall performance of the coupled process under the investigated reaction conditions was higher than for reported

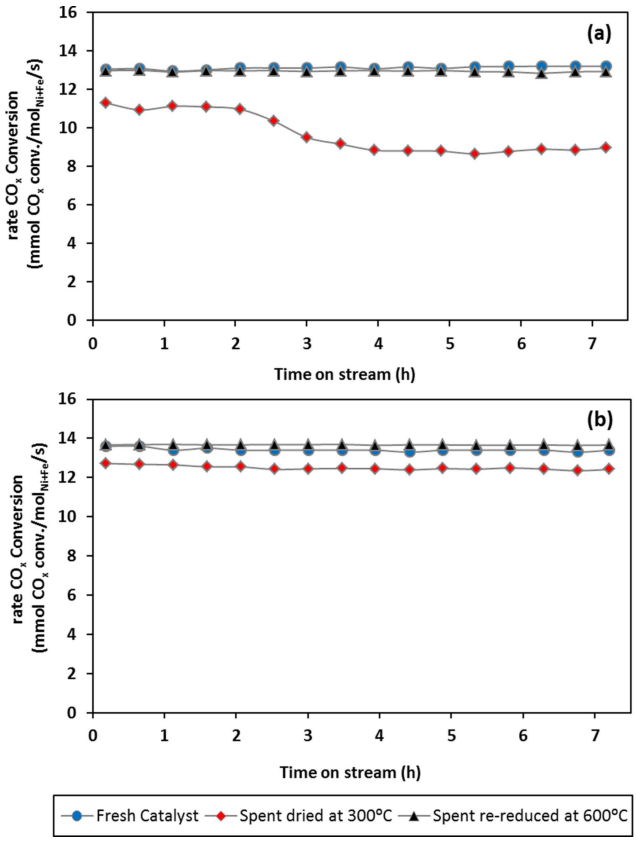

Figure 8. Regeneration tests over 20%Ni-2%Fe/(Mg,Al)O_x catalyst after the dynamic experiments. (a) 11% CO_2 + 5% CO and (b) 6% CO_2 + 10% CO. Reaction conditions were 300 °C, 1 atm, and GHSV = 5017 h^{-1}.

single electrochemical reactors used for direct generation of SNG from CO_2 and H_2O.[19,20] Though long term experiments are required, the preliminary results obtained under the dynamic conditions confirm that a coupled co-electrolysis and methanation can be considered as promising element of future sustainable and efficient energy storage technologies. Moreover, it should be pointed out that both the high-temperature SOEC module as well as the coupled P2G setup (design provided in Figure S1) constitute first prototypes, the functionality of which was demonstrated under different reaction conditions.

Concerning the co-electrolysis, we demonstrated that specifically desired syngas ratios [here H_2:(CO_2 + CO) = 4:1] can be obtained with several different experimental settings. Increasing the requirements on the co-electrolysis process by untightening a fixed power supply (dynamic conditions) is also feasible. The experimental settings are changed accordingly to the available power in such a way that still syngas in the desired ratio is produced for the downstream syngas methanation.

As far as syngas methanation is concerned, it was carried out at 300 °C and atmospheric pressure using a fixed-bed reactor. Initially, CO_2 and CO methanation were investigated as model reactions. Furthermore, the effect of water on the model reactions was studied to evaluate stability of the catalysts under an oxidizing atmosphere. Finally, representative feed mixtures that resemble the outlet from co-electrolysis under the dynamic nature of RE generation were used to evaluate the potential of the integration concept. While investigating the potential feed mixtures, we observed that higher water fractions (50% H_2O) lead to lower catalytic performance and enhanced catalyst deactivation. Similarly higher CO fractions also result in an increased selectivity to CO_2 (up to 10%), which is due to the water gas shift reaction in the presence of water (see Figure S7 in the Supporting Information). Therefore, in the presence of H_2O, appropriate amounts of CO_2 and CO are required for the selective production of SNG. It is known that in co-electrolysis, CO_2 conversion to CO is always lower than H_2O electrolysis; this fact can, therefore, help to provide a feed mixture appropriate for total methanation of CO_x selectively to SNG. Additionally, hydrotalcite-derived catalysts are known to possess a higher concentration of basic sites (due to the MgO) on the surface than conventional Ni on Al_2O_3 catalysts for CO_x methanation, which leads to enhanced adsorption and dissociation of CO_2. This might be also a reason for the hydrotalcite-derived Ni–Fe based catalyst to show higher activity and selectivity to SNG than the commercial Ni/Al_2O_3 catalyst. Therefore, we note that, if 20%Ni-2%Fe/(Mg,Al)O_x is used as a catalyst in the methanation step, decreasing the activation of CO_2 to CO in the co-electrolysis step is of importance for enhancing the selectivity to SNG. To sum up, the results obtained in CO_x methanation prove that a lower active metal loading (20 wt.% Ni and 2 wt.% Fe) is superior for higher SNG selectivity and activity compared to the commercial methanation catalyst with an active metal loading of about 75 wt.% Ni.

Considering regenerability of the 20%Ni-2%Fe/(Mg,Al)O_x catalyst in CO_x methanation, re-reduction was found to be a successful strategy to fully recover its initial activity. Post-

reaction characterization of the spent catalyst also showed no significant difference before and after the reaction. The average particle diameter estimated from STEM images (Figure 9) of reduced (13.7 ± 1.3 nm) and spent (12.9 ± 1.6 nm) 20 %Ni-2 %Fe/(Mg,Al)O_x catalyst does not show significant differences, indicating that sintering at reaction conditions was not the major origin of deactivation. Moreover, thermogravimetric (TG) analyses were performed under air to prove carbon deposition on the spent catalyst. As shown in Figure S6 (Supporting Information), the reduced (fresh catalyst) and spent (after the dynamic test with 11 % CO_2 + 5 % CO) does not show a significant weight loss at a higher temperature, which corresponds to the oxidation of carbon species. Hence, Ni oxidation in the presence of water was the only origin of catalyst deactivation after the dynamic experiments.

Conclusions

We demonstrate an integrated power-to-gas (P2G) process with a significantly enhanced rate of CO_x conversion and synthetic natural gas (SNG) selectivity by coupling high-temperature solid oxide electrolysis cell (SOEC) and syngas methanation. The novel P2G process reported here was built by coupling a SOEC module and a fixed-bed CO_x methanation reactor at optimized reaction conditions. The coupled system consists of a SOEC module based on a cathode-supported electrolysis cell using a Ni-8YSZ electrode in the co-electrolysis and a fixed bed reactor with 20 %Ni-2 %Fe/(Mg,Al)O_x as methanation catalyst, and up to 8 mmol CO_x conv. mol^{-1}_{Ni+Fe} s^{-1} rate of CO_x conversion was obtained with the feed mixture consisting of about 30 % H_2O. However, the activity was found to decrease significantly for 50 % H_2O. Oxidation of Ni^0 species in the presence of higher H_2O fractions is suggested as the origin of catalyst deactivation.

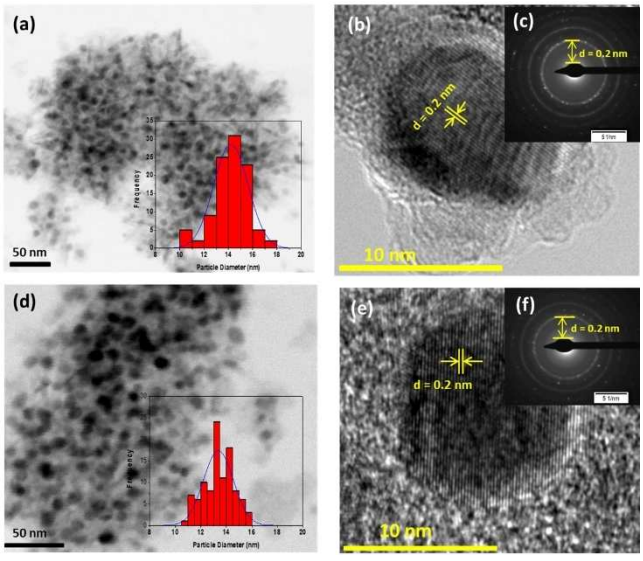

Figure 9. STEM, high-resolution (HR)TEM and diffraction images of 20 %Ni-2 %Fe/(Mg,Al)O_x catalyst: (a–c) freshly reduced at 600 °C and (d–f) spent after the dynamic test with 11 % CO_2 + 5 % CO.

Thus, re-reduction of the spent catalyst was found to be the most successful strategy to recover activity. Moreover, SNG selectivity was usually ≥ 90 %. Under the reaction conditions studied, full conversion of CO_2 to CO was not required from the co-electrolysis step to have a higher SNG selectivity in methanation. This is beneficial to the robustness of the overall efficiency of the integrated process even at lower renewable energy (RE) generation. Finally, we anticipate the higher rate of CO_x conversion and SNG selectivity in the integrated P2G process reported herein could be of considerable scientific interest and provide a new route for the design of clean and cost-effective RE storage methods.

Experimental Section

Details of the experimental methods used for both co-electrolysis and methanation are described in the Supporting Information.

Acknowledgements

We thank JARA-Energy Seed Fund (JARA-ENERGY MF 005-17) the Excellence Initiative by the German federal and state governments to promote science and research at German universities. The authors also gratefully acknowledge funding by the German Federal Ministry of Education and Research (BMBF) within the Kopernikus Project P2X: Flexible use of renewable resources – research, validation and implementation of 'Power-to-X' concepts (03SFK2A and 03SFK2A0-2). Open access funding enabled and organized by Projekt DEAL.

Conflict of Interest

The authors declare no conflict of interest.

Keywords: co-electrolysis · electrochemistry · heterogeneous catalysis · methanation · synthetic natural gas

[1] Global Status Report, *Renewables (REN 21)* **2018**.
[2] International Energy Agency (iea), Market analysis and forecast from 2018 to 2023 **2018**.
[3] Global Landscape of Renewable Energy Finance, *International Renewable Energy Agency, IRENA and CPI* **2018**.
[4] T. M. I. Mahlia, T. J. Saktisahdan, A. Jannifar, M. H. Hasan, H. S. C. Matseelar, *Renewable Sustainable Energy Rev.* **2014**, *33*, 532–545.
[5] A. Kumar, B. Sah, A. R. Singh, Y. Deng, X. He, P. Kumar, R. C. Bansal, *Renewable Sustainable Energy Rev.* **2017**, *69*, 596–609.
[6] M. Aneke, M. Wang, *Appl. Energy* **2016**, *179*, 350–377.
[7] M. Götz, J. Lefebvre, F. Mors, A. M. Koch, F. Graf, S. Bajohr, R. Reimert, T. Kolb, *Renewable Energy* **2016**, *85*, 1371–1390.
[8] S. Rönsch, J. Schneider, S. Matthischke, M. Schlüter, M. Götz, J. Lefebvre, P. Prabhakaran, S. Bajohr, *Fuel* **2016**, *166*, 276–296.
[9] S. R. Foit, I. C. Vinke, L. G. J. de Haart, R.-A. Eichel, *Angew. Chem. Int. Ed.* **2017**, *56*, 5402–5411; *Angew. Chem.* **2017**, *129*, 5488–5498.
[10] G. Gahleitner, *Int. J. Hydrogen Energy* **2013**, *38*, 2039–2061.
[11] P. Nikolaidis, A. Poullikkas, *Renewable Sustainable Energy Rev.* **2017**, *67*, 597–611.

[12] S. Schiebahn, T. Grube, M. Robinius, V. Tietze, B. Kumar, D. Stolten, *Int. J. Hydrogen Energy* **2015**, *40*, 4285–4294.
[13] G. A. Olah, *Angew. Chem. Int. Ed.* **2005**, *44*, 2636–2639; *Angew. Chem.* **2005**, *117*, 2692–2696.
[14] Y. Zheng, J. Wang, B. Yu, W. Zhang, J. Chen, J. Qiao, J. Zhang, *Chem. Soc. Rev.* **2017**, *46*, 1427–1463.
[15] Q. Fu, C. Mabilat, M. Zahid, A. Brisse, L. Gautier, *Energy Environ. Sci.* **2010**, *3*, 1382–1397.
[16] S. D. Ebbesen, X. Sun, M. B. Mogensen, *Faraday Discuss.* **2015**, *182*, 393–422.
[17] S. R. Foit, L. Dittrich, V. Vibhu, I. C. Vinke, R.-A. Eichel, L. G. J. de Haart, *ECS Trans.* **2017**, *78*, 3139–3147.
[18] L. Dittrich, M. Nohl, E. E. Jaekel, S. R. Foit, L. G. J. de Haart, R.-A. Eichel, *J. Electrochem. Soc.* **2019**, *166*, 971–975.
[19] L. Lei, T. Liu, S. Fang, J. P. Lemmon, F. Chen, *J. Mater. Chem. A* **2017**, *5*, 2904–2910.
[20] L. Chen, F. Chen, C. Xia, *Energy Environ. Sci.* **2014**, *7*, 4018–4022.
[21] Y. Luo, Y. Shia, W. Lia, N. Cai, *Energy Convers. Manage.* **2018**, *165*, 127–136.
[22] J. Hartvigsen, S. Elangovan, L. Frost, A. Nickens, C. Stoots, J. O'Brien, J. S. Herring, *ECS Trans.* **2008**, *12*, 625–637.
[23] E. Giglio, A. Lanzini, M. Santarelli, P. Leone, *J. Energy Storage* **2015**, *1*, 22–37.
[24] E. Giglio, A. Lanzini, M. Santarelli, P. Leone, *J. Energy Storage* **2015**, *2*, 64–79.
[25] N. Fujiwara, S. Tada, R. Kikuchi, *Sustainable Energy Fuels* **2020**, *4*, 2691–2706.
[26] S. H. Jensen, C. Graves, M. Mogensen, C. Wendel, R. Braun, G. Hughes, Z. Gao, S. A. Barnett, *Energy Environ. Sci.* **2015**, *8*, 2471–2479.
[27] C. Bina, Y. S. Hajimolana, V. Venkataraman, M. Ni, P. V. Aravind, *Energy Procedia* **2019**, *158*, 2077–2084.
[28] J. P. Stempien, M. Ni, Q. Sun, S. H. Chan, *Energy* **2015**, *81*, 682–690.
[29] E. Giglio, F. A. Deorsola, M. Gruber, S. R. Harth, E. A. Morosanu, D. Trimis, S. Bensaid, R. Pirone, *Ind. Eng. Chem. Res.* **2018**, *57*, 4007–4018.
[30] C. Mebrahtu, F. Krebs, S. Perathoner, S. Abate, G. Centi, R. Palkovits, *Catal. Sci. Technol.* **2018**, *8*, 1016–1027.
[31] C. Mebrahtu, PhD thesis, RWTH Aachen University (DE) and University of Messina (IT) **2018**.
[32] S. D. Senanayake, J. Evans, S. Agnoli, L. Barrio, T.-L. Chen, J. Hrbek, J. A. Rodriguez, *Top. Catal.* **2011**, *54*, 34–41.
[33] J. YangLim, J. McGregor, A. J. Sederman, J. S. Dennis, *Chem. Eng. Sci.* **2016**, *152*, 754–766.
[34] S. Hwang, U. G. Hong, J. Lee, J. H. Baik, D. J. Koh, H. Lim, I. K. Song, *Catal. Lett.* **2012**, *142*, 860–868.
[35] X. Su, J. Xu, B. Liang, H. Duan, B. Hou, Y. Huang, *J. Energy Chem.* **2016**, *25*, 553–565.
[36] Y. Tang, Y. Kobayashi, C. Tassel, T. Yamamoto, H. Kageyama, *Adv. Energy Mater.* **2018**, *8*, 1800800.
[37] C. Mebrahtu, S. Perathoner, G. Giorgianni, S. Chen, G. Centi, F. Krebs, R. Palkovits, S. Abate, *Catal. Sci. Technol.* **2019**, *9*, 4023–4035.

Manuscript received: December 19, 2020
Revised manuscript received: April 12, 2021
Accepted manuscript online: April 26, 2021
Version of record online: May 7, 2021